NEUTRON SHIELDING MATERIAL CONTAINING BASALT-BORON FIBERS AND OSA FOR SPENT NUCLEAR FUEL CONTAINER, NUMERICAL MODELLING

Iryna Romanenko[1], Iveta Novakova[2], Riho Motlep[3], Volodymyr Gulik[3], Andrejs Krasnikovs[1], Mindaugas Vaisnoras[4]
[1]Riga Technical University, Latvia;
[2]Arctic University of Norway, Norway;
[3]University of Tartu, Estonia;
[4]Lithuanian Energy Institute, Lithuania
romanenko.iryna74@gmail.com, iveta.novakova@uit.no, riho.motlep@ut.ee, volodymyr.gulik@gmail.com, andrejs.krasnikovs@rtu.lv, mindaugas.vaisnoras@lei.lt

Abstract. Nuclear power plants and research purposed reactors produce spent nuclear fuel, which leads to a need for safe spent fuel management and radiation protection. Traditionally, concrete with the addition of different aggregates has been the primary material for shielding against radiation and is used also for transport and storage of radioactive waste. Despite these applications, there is still a need to develop new composite materials that will preserve the radiation shielding properties of concrete, while offering superior mechanical and also cost effective benefits. This article investigates the radiation shielding properties of HI-STORM containers, made of a new composite material, and reinforced with basalt-boron fibre for human and environment protection. In the concrete recipe, part of the cement is replaced by oil shale ash with cementitious characteristics. The formulation of concrete reinforced with basalt-boron fibre (with the addition of 6% boron oxide) is presented. Oil shale ash (OSA) is a class-C fly ash, a by-product in the energy production process. OSA can be used as a partial replacement to cement in concretes, thanks to its cement-like qualities and low carbon content, which contributes to a reduction in the overall CO_2 footprint of concrete. In our investigated concrete mixes 5 to 35% of cement was replaced by OSA (Electrostatic Precipitator Ash) coming from Auvere (Estonia) thermal power plant. Using the Monte Carlo method, the Serpent code was used to simulate the passage of neutron radiation through a composite material to assess its biological shielding properties. It is shown that the addition of basalt-boron fibre to concrete improves the protective properties of biological shielding against neutron radiation.

Keywords: HI-STORM, basalt-boron fibre, biological protection, spent nuclear fuel.

Introduction

Over the past decades, nuclear power has proven its efficiency and has become an integral part of the energy mix alongside other types of energy. As of 2023, 436 nuclear reactors were operating in 32 countries [1]. Over the next few decades, it is anticipated that global electricity consumption will increase significantly. Nuclear power industry generates waste, notably in the form of spent nuclear fuel (SNF). Hence, ensuring the safe management and storage of spent nuclear fuel is of high priority. An important factor in the safe and long-term storage of spent nuclear fuel is the preservation of concrete's structural integrity. Concrete is the most common structural material used in the nuclear power industry to protect against ionising radiation. Usually, various aggregates are added to concrete to preserve the radiation properties of concrete and improve its mechanical characteristics.

Over the past decades, many scientists have investigated the properties of concrete with various admixtures [2-10]. Good material integrity results were obtained observing concretes with short fibers – fiberconcretes [11-12]. At the moment, there is still a need to develop new composite materials that would meet all the needs for safe storage and management of spent nuclear fuel. In this study we consider the storage of spent nuclear fuel from VVER 1000 reactors in the HI-STORM 190 container. We model fast neutron transfer through four types of concrete with the addition of basalt-boron fibre (BBF) and oil shale ash (OSA) to the concrete. HI-STORM 190 containers are designed to shield radioactive materials by incorporating concrete between two metal shells. Boron is used since it has a large neutron cross section, and is used for absorption neutrons in concrete material.

Materials and methods

The Monte Carlo code Serpent version 2.1.31 facilitates the simulation of the shielding properties of HI-STORM 190 containers for spent nuclear fuel (SNF). The developed model allows for calculating neutron transfer from spent fuel assemblies through the canister, and enables the assessment of both the effectiveness of a new composite material and its biological shielding properties.

DOI: 10.22616/ERDev.2024.23.TF109

When creating the computational Serpent model, we used the geometric characteristics available in open sources [13-15]. The main components of the simplified computational model are shown in Table 1. In the model of the HI-STORM 190 container, certain simplifications were implemented. Specifically, the lid, bottom, and air circulation openings were not included in the model. This simplification substantially reduces the number of cells and calculation time required.

Table 1

Main geometrical characteristics of the HI-STORM 190 container

Element	Size, cm
Inner radius of the basket MPC-31	93
Outer radius of the basket MPC-31	96
Inner radius of the container HI-STORM 190	103
Outer radius of the container HI-STORM 190	178
Height of the container HI-STORM 190	580
Metal thickness of the container HI-STORM 190	2
Fuel zone is located at a height	49
Height of the fuel zone	355
Height from the fuel zone to the container HI-STORM 190	176

The HI-STORM 190 multi-purpose container (MPC) has a rather complex structure. The container is designed for long-term storage of 31 VVER 1000 spent fuel assemblies. The HI-STORM 190 is a ventilated vertical container consisting of an outer and an inner steel cask with the space between them filled with concrete that serves as a biological shield. In the centre of the HI-STORM 190 container is a MPC -31holder loaded with 31 VVER-1000 fuel assemblies. The central fuel assembly is located in the centre of the container. The spacing of fuel assemblies in MPC -31 is 25.32 cm. For the sake of simplicity, uranium dioxide with 4.34% enrichment and a density of 10.22 $g \cdot cm^{-3}$ is used as the spent fuel, which serves as a source of neutron radiation. The spectrum of the neutron radiation source with a breakdown by energy groups used in this model is shown in Table 2. A Russian-made TVZA 438MT cassette with a burnup of 55000 [$MW \cdot day \cdot (kgU)^{-1}$] and an endurance of 6 years was modelled as a spent fuel assembly (SFA). The neutron sources used for the neutron transfer calculation were the cells, where the fuel assemblies are located in MPC -31.

Table 2

Spectrum of the neutron source

No	Upper limit of the energy bin, MeV	Energy bin weight, rel. units
1	1.00E-01	0.00000E + 00
2	4.00E-01	7.39020E-02
3	9.00E-01	1.60473E-01
4	1.40E + 00	1.60473E-01
5	1.85E + 00	1.28378E-01
6	3.00E + 00	2.39302E-01
7	6.43E + 00	2.16779E-01
8	2.00E + 01	2.06926E-02

The SRC card was used to simulate neutrons emitted from SFA. To specify an external neutron source in the Serpent code, it is necessary to specify also the geometry of the external source, the energy of the emitted particles and the radiation intensity. Neutron source parameters (partitioning into energy bins and corresponding intensities) were obtained by a separate calculation simulating burnup for 6 years in a nuclear reactor and storage in the cooling pool for 5 years. The neutron sources used for the neutron transfer calculation were the cells containing SFA in MPC-31 (see Fig. 1). For one calculation, 100 million neutrons divided into 200 batches were modelled. The current libraries of evaluated nuclear data - ENDF/B-VII - were used. The particle radiation vector is directed horizontally from the centre of the container to the periphery. Fission and time-cutting reactions were excluded. Absorbing boundary conditions were used (this means that when a neutron reaches the outer boundary of the model, it is excluded from the calculation).

To measure the neutron flux, the volumetric regions (“detectors”) in which neutrons were captured were modelled in the developed model. Particle detection was performed by the Serpent code using eight cylinders located at the level of the fuel column SNF. Seven detectors are located in the concrete itself (between the outer and inner shell), and the eighth detector is located behind the concrete. The detector is a cylinder with a radius of 5 cm, where data on the required neutron-physical characteristics are collected. The detectors were placed at the locations with coordinates shown in Table 3. The origin in the presented model is located in the centre of the cylindrical system on the lowest surface of the model (the boundary of the canister and the foundation where it stands).

Table 3

Coordinates of detectors

Detector identification	X, cm	Y, cm	R, cm	Z_1, cm	Z_2, cm
det1	108	0	5	49	402
det2	118.5	0	5	49	402
det3	129	0	5	49	402
det4	139.5	0	5	49	402
det5	150	0	5	49	402
det6	160.5	0	5	49	402
det7	171	0	5	49	402
det8	183	0	5	49	402

The neutron flux was assessed both with the help of cylindrical detectors placed in the concrete itself and with the help of a detector placed on the outer surface of the HI - STORM 190 container.

An explanation of the Serpent syntax, including the functions “surf”, “cell”, “mat”, and so on, is given in full in the literature [16].

Experimental samples were also produced in order to check, how cement replacement by OSA and addition of basalt boron fibers are changing the concrete (more precisely – fiberconcrete) radiation shielding capacity. Four types of fiberconcretes were used as the biological protection material in the HI-STORM 190 container (described in detail in [17]). Fiberconcrete mixes were prepared and cast into cubes measuring 10x10x10 cm. Short, 24 mm long basalt-boron fibres with 6% boron oxide (BBF), in different concentrations were mixed with other concrete ingredients: cement, OSA, dolomite gravels, sand (different granulometry), dolomite flour, plasticizer and Elkem-microsilica. Ingredient characteristics and proportions for the considered concretes used for the design model are presented in Table 4.

Table 4 [17]

Material compositions and densities of the considered concretes

No	Parameter	A	B	C	D
1	Density, $g \cdot cm^{-3}$	2.301	2.303	2.251	2.339
2	Weight fraction of cement *, %	9.52	8.69	7.40	8.68
3	Weight fraction of sand, %	47.27	40.42	65.97	40.36
4	Weight fraction of rubble **, %	26.26	31.40	2.36	31.35
5	Weight fraction of water, %	8.21	7.65	9.82	7.45
6	Weight fraction of dolomite flour %	7.88	5.69	9.42	5.68
7	Weight fraction of oil shale ash, %	0	4.67	3.99	4.66
8	Weight fraction of plasticiser, %	0,30	0,59	0.35	0.59
9	Weight fraction of microsilica, %	0	0.20	0	0.20
10	BBF (24 mm), %	0.58	0.69	0.69	1.03

* - cement used CEM II A-LL 42,5N [17]

**- dolomite used [17]

Fiberconcrete mix A is the material with the smallest amount of BBF and without OSA. Fiberconcrete mix D is fiberconcrete with the highest BBF concentration and cement partially replaced by OSA. Fiberconcretes B and C have intermediate amount of OSA and BBF.

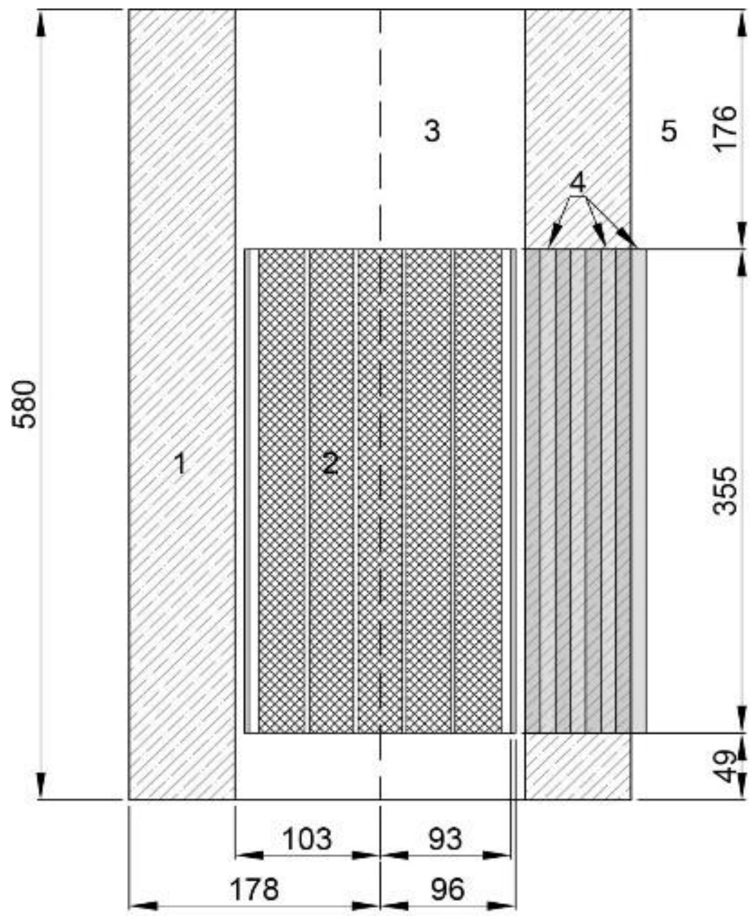

Fig 1. **Schematic representation of the central section of a simplified Serpent model:**
1 – concrete biological protection; 2 – MPC; 3 – air; 4 – particle detection zones; 5 – air

Results and discussion

As a result of the modelling, a simplified model of the HI-STORM 190 canister with loaded SFA was developed. For each of the four types of concrete, the neutron flux in 8 detectors was found. Neutron spectra were obtained in all detectors for different types of concrete. In addition, the total neutron flux in all detectors for different types of concrete was obtained. The total neutron flux is shown in Fig. 2. All neutron spectra are presented per neutron of an external source. In other words, the presented spectra give a qualitative picture of the neutron distribution by energy in different parts of the concrete.

The results of the calculation of the total neutron flux depending on the location of the detector are presented in Table 6. The results show that:

1. All types of concrete are similar and reduce the neutron flux from SNF.
2. The considered types of concrete are characterised by increased (compared to conventional concrete [4]) neutron absorption over the entire energy spectrum.
3. The addition of OSA shows a slight deterioration in the neutron absorption capacity compared to type A concrete.
4. As it can be seen from the results of the study, concrete type C (water content 9.82% and BBF 0.69%) at the detector 8 (outside the HI-STORM 190 container) shows almost the same neutron absorption capacity compared to concrete type A (water content 8.21% and BBF 0.58%).
5. Other types of concrete (B and D) with lower water content (>8%) show worse results compared to type A (1.21 and 1.09 times, respectively).

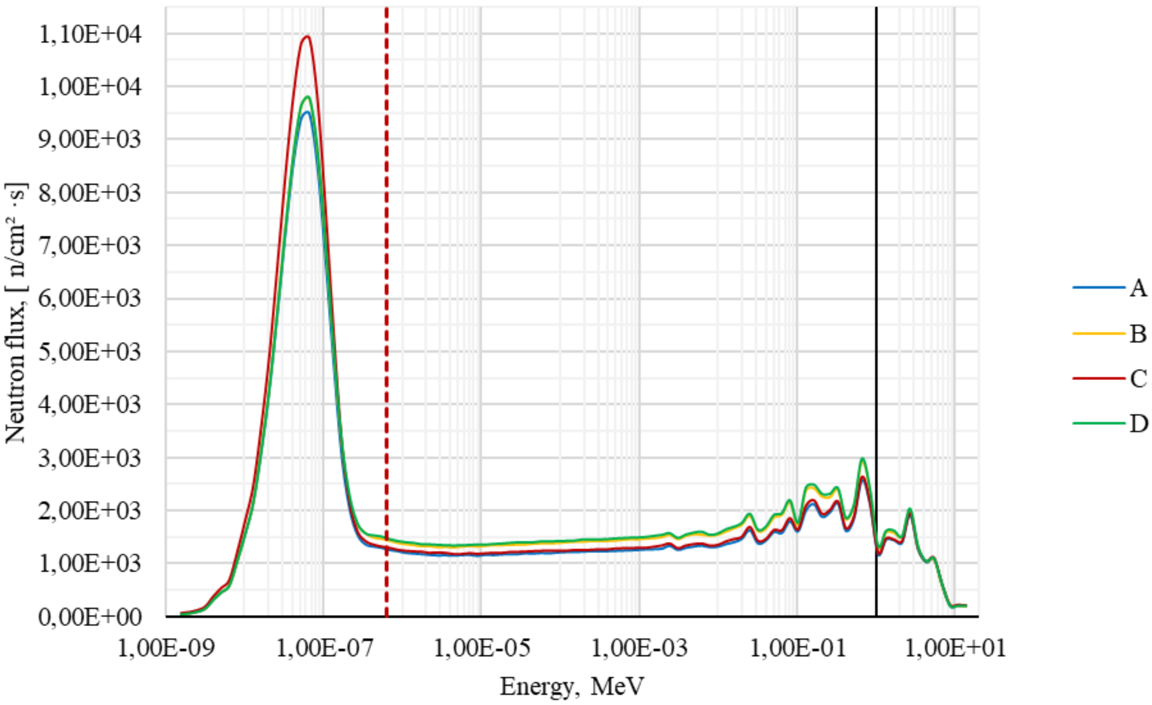

Fig. 2. **Total neutron flux by energy**

Table 6

Total neutron flux in the detection zones

Detector	**Type A**	**Type B**	**Type C**	**Type D**
	Total neutron flux in detection zone, $1/(cm^2 \cdot s)^{-1}$			
det 1	1.16E + 05	1.19E + 05	1.20E + 05	1.20E + 05
det 2	4.67E + 04	5.31E + 04	5.19E + 04	5.40E + 04
det 3	1.41E + 04	1.83E + 04	1.68E + 04	1.88E + 04
det 4	3.96E + 03	5.68E + 03	4.88E + 03	5.91E + 03
det 5	1.18E + 03	1.80E + 03	1.47E + 03	1.86E + 03
det 6	3.78E + 02	5.89E + 02	4.95E + 02	6.06E + 02
det 7	1.18E + 02	1.62E + 02	1.53E + 02	1.81E + 02
det 8	1.51E + 01	1.83E + 01	1.54E + 01	1.65E + 01

Conclusions

After modelling a simplified model of the HI-STORM 190 container and performing calculations, the results obtained were analysed in terms of neutron flux attenuation in modified concrete types. Based on this, the following conclusions can be drawn.

- The results show that the studied aggregates are promising materials for use in radiation protection.
- Basalt-boron fibers are increasing neutron absorption over the entire energy spectrum. More intensively it happens at the middle spectrum part (see data for the concrete D in Fig. 2).
- It is advisable to continue the selection of concrete compositions in order to obtain the optimal ratio of water, OSA and BBF in the concrete mixture while maintaining other indicators.

Acknowledgments

The authors acknowledge for financial support from the Baltic Research Programme project No. EEA-RESEARCH-165 “Innovation in concrete design for hazardous waste management applications” under the EEA Grant of Iceland, Liechtenstein and Norway Project Contract No. EEZ/BPP/VIAA/2021/6.

Author contributions

All authors have read and agreed to the published version of the manuscript.

References

[1] Nuclear power plants in the world 2023, Statista. Accessed: Feb. 02, 2024. [online] [11.02.2024] Available at: https://www.statista.com/statistics/267158/number-of-nuclear-reactors-in-operation-by-country/

[2] Pastsuk V. et al., Selection of basalt fiber with resistance to concrete alkaline environment, SN Appl. Sci., vol. 2, no. 11, p. 1842, Oct. 2020, DOI: 10.1007/s42452-020-03677-z.

[3] Chuvashov Y., Jashchenko O., Diduk I., Gulik V. The Investigation of Fiber Surface Condition from Basalt-like Rocks for Enhanced Industrial Applications, J. Nat. Fibers, vol. 19, no. 8, pp. 2953-2962, Aug. 2022, DOI: 10.1080/15440478.2020.1838987.

[4] Romanenko I., Holiuk M., Nosovsky A., Vlasenko T., Gulik V., New Composite Material Based on Heavy Concrete and Basalt-Boron Fiber for Neutron Radiation Shielding Properties, Nuclear and Radiation Safety, no. 2(82), Art. no. 2(82), Jun. 2019, DOI: 10.32918/nrs.2019.2(82).04.

[5] Zorla E. et al.Optimization of basalt fiber in concrete composite for industrial application in Estonia, Fresenius Environ. Bull., vol. 25, pp. 355-364, Jan. 2016.

[6] Singh V. P., Badiger N. M. Investigation on radiation shielding parameters of ordinary, heavy and super heavy concretes, Nucl. Technol. Radiat. Prot., vol. 29, no. 2, pp. 149-156, 2014.

[7] İçelli O., Yalçın Z., Okutan M., Boncukçuoğlu R. Determination of photon energy absorption parameters for pellet waste, trommel sieve waste and original tincalconite, Ann. Nucl. Energy, vol. 47, pp. 38-45, Sep. 2012, DOI: 10.1016/j.anucene.2012.03.028.

[8] Singh V. P., Badiger N. M. Gamma Photon Exposure Buildup Factors for Some Spin Ice Compounds Using G-P Fitting Method, J. Nucl. Phys. Mater. Sci. Radiat. Appl., vol. 2, no. 2, Art. no. 2, Feb. 2015, DOI: 10.15415/jnp.2015.22013.

[9] Malkapur S. M., Satdive H., Narasimhan M. C., Karkera N. B., Goverdhan P., Sathian V. Effect of mix parameters and hydrogen loading on neutron radiation shielding characteristics of latex modified concrete mixes, Prog. Nucl. Energy, vol. 83, pp. 8-12, Aug. 2015, DOI: 10.1016/j.pnucene.2015.02.010.

[10] Ipbüker C., Nulk H., Gulik V., Biland A., Tkaczyk A. H. Radiation shielding properties of a novel cement-basalt mixture for nuclear energy applications, Nucl. Eng. Des., vol. 284, pp. 27-37, Apr. 2015, DOI: 10.1016/j.nucengdes.2014.12.007.

[11] Lusis V., Annamaneni K.K., Krasnikovs A. Concrete Reinforced by Hybrid Mix of Short Fibers under Bending, Fibers, Open Access, vol. 10, Issue 2, Feb. 2022, Article no. 11, DOI: 10.3390/fib10020011

[12] Macanovskis A. et al. Composite fibers in concretes with various strengths, ACI Materials Journal, vol. 115, Issue 5, pp. 647-652, Sep.-Oct. 2018, DOI: 10.14359/51702343

[13] Alyokhina S., Dybach O., Kostikov A., Dimitriieva D. Prediction of the maximum temperature inside container with spent nuclear fuel, Ядерна Та Радіаційна Безпека, no. 2(78), Art. no. 2(78), Jun. 2018, DOI: 10.32918/nrs.2018.2(78).05.

[14] Будівництво Централізованого сховища відпрацьованого ядерного палива | PPT. (Construction of the Centralised Spent Fuel Storage Facility). Accessed: Feb. 02, 2024. [online] [11.02.2024]. Available at: https://www.slideshare.net/Ukrainian_Nuclear_Society/ss-117592614 (In Russian)

[15] ОТРАБОТАВШЕЕ ЯДЕРНОЕ ТОПЛИВО: международный опыт использования и перспективы его внедрения в Украине.(Spent nuclear fuel: international experience of use and prospects of its introduction in Ukraine). SlideShare. Accessed: Feb. 02, 2024. [online] [11.02.2024]. Available at: https://www.slideshare.net/ssusercfa346/ss-46349873 (In Russian)

[16] Leppänen J., Pusa M., Viitanen T., Valtavirta V., Kaltiaisenaho T. The Serpent Monte Carlo code: Status, development and applications in 2013, Ann. Nucl. Energy, vol. 82, pp. 142-150, Aug. 2015, DOI: 10.1016/j.anucene.2014.08.024.

[17] Tohver H. et al. Assessing shielding material Performance: Benchmarking of Monte Carlo codes for oil shale and Basalt-Boron fiber concretes, Nucl. Eng. Des., vol. 417, p. 112811, Feb. 2024, DOI: 10.1016/j.nucengdes.2023.112811.